High-throughput detection of neutralizing antibodies to SARS-CoV-2 variants using flow cytometry

Xiaohan Zhang[1,2*], Yajie Wang[4*], Mansheng Li[2*], Haolong Li[3*], Xiaomei Zhang[2], Xingming Xu[2], Di Hu[5], Te Liang[2], Yunping Zhu[2], Yongzhe Li[3#], Bingwei Wang[1#] and Xiaobo Yu[2#]

Affiliations

[1]College of Medicine and Integrated Medicine, Nanjing University of Chinese Medicine, Nanjing 210023, China.

[2]State Key Laboratory of Proteomics, Beijing Proteome Research Center, National Center for Protein Sciences-Beijing (PHOENIX Center), Beijing Institute of Lifeomics, Beijing, 102206, China.

[3]Department of Clinical Laboratory, Peking Union Medical College Hospital, Chinese Academy of Medical Science & Peking Union Medical College, Beijing 100730, China.

[4]Department of Clinical Laboratory, Beijing Ditan Hospital, Capital Medical University, Beijing 100015, China.

[5]ProteomicsEra Medical Co., Ltd., Beijing, 102206, China

[*]These authors contributed equally to this work.

[#]Correspondence to yuxiaobo@mail.ncpsb.org (X.Y.), bingweiwang@njubw.edu.cn (B.W.) and yongzhelipumch@126.com (Y. L).

Abstract

Detecting neutralizing antibodies (NAbs) to SARS-CoV-2 variants is crucial for controlling the spread of COVID-19. In this work, we developed a high-throughput assay for the broad systematic examination of NAbs to eleven SARS-CoV variants of concern (VOCs), which include D614G, Alpha, Beta, Gamma, Delta, Kappa, and Omicron sub-lineages BA.1, BA.2, BA.3, BA.4, and BA.5. The assay is cost-effective, reliable, 35-fold more sensitive than Luminex technology, and can include the new variants during SARS-CoV-2 evolution. Importantly, our results highly correlated with a commercial IgG serological assay (R = 0.89) and cPass, a U.S. FDA-approved surrogate virus neutralization test (sVNT) assay (R = 0.93). With our high-throughput NAb platform, we constructed a comprehensive overview of the interactions between SARS-CoV-2 VOCs' Spike trimer proteins and ACE2 receptors, leading to the identification of a monoclonal Ab with broad neutralizing activity. Furthermore, when compared to the D614G variant, we found that the serum NAbs elicited by the third dose vaccine (administered after 28 days) demonstrated decreased inhibition to multiple SARS-CoV-2 variants, including Gamma (0.94×), Alpha (0.91×), Delta (0.91×), Beta (0.81×), Kappa (0.81×), BA.2 (0.44×), BA.1 (0.43×), BA.3 (0.41×), BA.5 (0.35×) and BA.4 (0.33×), in cohort of 56 vaccinated individuals. Altogether, our

proteomics platform proves to be an effective tool to detect broad NAbs in the population and aid in the development of future COVID-19 vaccines and vaccination strategies.

Keywords

SARS-CoV-2, flow cytometry, neutralization, antibody, COVID-19

Introduction

The ongoing coronavirus 2019 (COVID-19) pandemic, caused by the severe acute respiratory syndrome coronavirus 2 (SARS-CoV-2), remains a public health concern worldwide. This is primarily attributed to the continuous evolution of the virus and its persistent transmission across global populations[1]. For instance, over ten SARS-CoV-2 variants of concern (VOCs) have appeared, and these VOCs have the potential to reduce the immune response[2]. According to reports, 17.13% (95%CI, 7.55–26.71%) of asymptomatic infected individuals may have long-term health consequences [3], which may include symptoms such as fatigue, brain fog, dizziness, gastrointestinal symptoms, as well as others [4].

Neutralizing antibodies (NAbs) of SARS-CoV-2 are a subset of antibodies that block viral entry by inhibiting the interaction between the SARS-CoV-2's surface protein, Spike, and the host cell's receptor,

angiotensin-converting enzyme 2 (ACE2). Such NAbs can be produced following COVID-19 vaccination or SARS-CoV-2 infection. Identifying SAR-CoV-2 NAbs is critical for assessing vaccine efficacy, evaluating individual and population immunity, monitoring variant susceptibility, and information public health measures to control the spread of COVID-19. However, traditional methods of NAb detection, such those that use a live virus or a pseudovirus-based neutralization assay, are slow, expensive, carry a potential risk of infection, and may require specialized biosafety level 3 (BSL3) facilities [5-8].

As an alternative approach, enzyme-linked immunosorbent assay (ELISA) can perform the *in vitro* neutralizing testing using purified Spike, ACE2, or Spike's receptor-binding domain (RBD) that interacts directly with ACE2 during viral entry. Several commercial ELISA-based surrogate virus neutralization tests (sVNT) have been developed, including TECO sVNT (TECO Medical) and cPASS sVNT (GenScript), which have been approved by the United States' (U.S.) Food and Drug Administration (FDA) or received Conformite Europeenne (CE) marking for use in the European Union [9, 10]. Unfortunately, ELISA-based methods only detect a single variant at a time, making them a time-consuming option when multiple SARS-CoV-2 variants are analyzed [6].

To address this concern, Fenwick *et al.* developed a multiplexed *in-vitro* quantitative neutralization assay using Luminex technology in 2021. The assay enables the detection of NAbs targeting various Spike mutations, including D614G, D614G plus M153T, N439K, S477N, S477R, E484K, S459Y, N501T, N501Y, K417N, 60-70, P681H, Y453F, and their combinations. The results obtained from this assay correlated with pseudovirus neutralization (R^2=0.65) and live virus infection (R^2 = 0.825) assays [7].

In a similar vein, Lynch et al. developed a multiplexed surrogate virus neutralization test (plex-sVNT) for detecting NAbs to seven SARS-CoV-2 variants, namely, wild type, Alpha, Beta, Gamma, Delta, Kappa, and Epsilon. The results highly correlated (> 96%) with those obtained from a plaque reduction neutralization test (PRNT)[8].

However, it should be noted that these technologies have limitations as they require access to specific Luminex and Bio-Rad instruments, thereby restricting their use to specific laboratories. Moreover, some recent Omicron variants have not been accessible for analysis using these methods to date[11].

In this work, we developed a high-throughput broad neutralizing antibody (bNAb) assay that enables the systematic detection of NAbs to eleven SARS-CoV-2 VOCs that is reliable, cost-effective, sensitive, and used with a standard flow cytometer [12]. These variants include

D614G, Alpha, Beta, Gamma, Delta, Kappa, Omicron BA.1, Omicron BA.2, Omicron BA.3, Omicron BA.4, and Omicron BA.5. We conducted a comparative analysis of NAb detection using our SARS-CoV-2 bNAb assay with commercial ELISA-based serology and U.S. FDA-approved cPASS sVNT assays. Furthermore, we explored the applications of the SARS-CoV-2 bNAb assay for screening therapeutic Abs, assessing their neutralizing activity SARS-CoV-2. Finally, we analyzed the broad responses of serological NAbs to SARS-CoV-2 VOCs in individuals who received the third dose of either the inactivated vaccine (Sinovac-CoronaVac) or the recombinant subunit vaccine (ZF2001) for COVID-19.

Results

Schematic illustration of SARS-CoV bNAb assay

In the SARS-COV-2 bNAb assay, illustrated schematically in Figure 1A, the trimerized Spike protein of six non-Omicron variants (D614G, Alpha, Beta, Kappa, Gamma, Delta) and five Omicron variants (BA.1, BA.2, BA.3, BA.4, BA.5) were expressed from human embryonic kidney 293 (HEK293) cells, purified, and coupled to the fluorescence-encoded magnetic beads, as previously reported [7, 13]. Prior to the assay, the resulting beads were blocked and incubated with the samples containing NAbs. The binding of Abs to the Spike protein blocks its

interaction to the biotinylated ACE2 receptor that is coupled to streptavidin-phycoerythrin (SA-PE). The inhibition rate (%) was the percentage of the Spike-ACE2 interaction signal in the serum samples with NAbs compared to the control without NAbs.

The sensitive detection of Spike-ACE2 interactions is essential for assessing the presence of NAbs in clinical samples. To address this requirement, we coupled the Spike protein from six SARS-CoV-2 VOCs (D614G, Alpha, Beta, Kappa, Delta, Omicron BA.1) onto fluorescent magnetic beads from Luminex and Shenzhen Wellgrow Technology Co., Ltd. ("Wellgrow"), and then incubated with different concentrations of ACE2. Magnetic beads with the SARS-CoV-2 nucleocapsid (N) protein, rather than the Spike protein, was employed as the negative control. The binding signals were measured using Luminex-200 and Wellgrow flow cytometry. Notably, the fluorescent signal intensity was much higher with the Wellgrow platform than the Luminex platform when ACE2 concentrations ranged from 0.01 μg/mL to 100 ng/mL (Figure 1B and Supplementary Figure 1).

Furthermore, we calculated the sensitivity or the lowest detection limit (LOD) of each method, in which the LOD was equal to the signal of the buffer control plus ten standard deviations (Figure 1C). The data showed that the average LOD of our assay using the Wellgrow platform was 35.89±57.8 [-21.91~93.69]-fold higher than the Luminex

platform for all variants (D614G, Alpha, Beta, Kappa, Delta, Omicron BA.1). Therefore, we selected the Wellgrow platform as the proteomics platform for the SARS-CoV-2 bNAb assay in this study.

Mapping Spike-ACE2 interactions of SARS-CoV-2 VOCs

Using our platform, we conducted a systematic investigation of the interactions between ACE2 and Spike trimer proteins from eleven SARS-CoV-2 VOCs. This was achieved by incubating a bead array with different concentrations of ACE2 (Figure 2). The results demonstrated that the fluorescent signals from the Spike trimer proteins increased with increasing concentrations of ACE2 (Figure 2A), indicating the formation of Spike-ACE2 complexes on the beads.

Spike mutations were found to influence the interaction dynamics. At the maximal concentration of 10 μg/mL ACE2, Alpha and Delta variants exhibited the highest signals, followed by Beta, BA.4, BA.5, D614G, Gamma, BA.1, BA.2, and Kappa, with BA.3 showing the lowest signal. In contrast, the N protein, used as a negative control, consistently displayed the lowest signal regardless of ACE2 concentration.

To further assess the binding affinity, we calculated the half-maximal effective concentration (EC50) using the standard curve for each SARS-CoV-2 variant (Figure 2B). The results showed that

Omicron BA.1 has the highest binding affinity with an EC50 of 0.2913 µg/mL, followed by Beta (0.2913 µg/mL), Delta (0.3415 µg/mL), Omicron BA.4 (0.3592 µg/mL), Gamma (0.3833 µg/mL), Alpha (0.394 µg/mL), Kappa (0.3983 µg/mL), Omicron BA. 2 (0.4307µg/mL), Omicron BA. 5(0.4593 µg/mL), D614G (0.5279 µg/mL), and Omicron BA.3 (1.283 µg/mL). The results are in accordance with surface plasma resonance data in which BA.1 has the strongest interaction with ACE2 with a dissociation constant (K_D) of 2.10 nM, followed by BA.2 (2.21 nM) and D614G (5.20 nM) [14]. Similar results were obtained by Mahalingam et al., who used ELISA to determine the EC50 of ACE2 to Spike Omicron (0.38 nM), Delta (0.48 nM), and wild type (2.28 nM)[15]. Collectively, our data provide a comprehensive landscape of Spike trimer-ACE2 interactions for SARS-CoV-2 VOCs, as classified by the U.S. Centers for Disease Control and Prevention (CDC) (https://www.cdc.gov/coronavirus/2019-ncov/variants/variant-classifications.html). It should be noted that the Epsilon variant was not included in this work due to the unavailability of purified Spike trimer protein.

Comparison of SARS-CoV-2 bNAb assay to ELISA and sVNT assays

To assess the reliability of the SARS-CoV-2 bNAb assay, we compared the SARS-CoV-2 bNAb assay to an ELISA that was used to detect

anti-Spike IgG antibodies[16]. The results showed a high correlation between the levels of D614G NAbs detected using our SARS-CoV-2 bNAb assay and the anti-Spike IgG antibodies obtained by the ELISA [R = 0.89, p-value (p) < 2.2 e-16] in a cohort of 75 individuals (Figure 3A).

Next, we compared the NAb results obtained from the SARS-CoV-2 bNAb assay to those obtained from the FDA-approved cPass sVNT test [6, 9]. The data obtained using the SARS-CoV-2 bNAb assay and cPass sVNT test demonstrated a higher correlation to each other (R = 0.93, p < 2.2 e-16) compared to the assay using Luminex technology (R=0.85)[17]. The positive percent agreement (PPA) was 92.7% (80.1%-98.5%) and the negative percent agreement (NPA) was 94.1% (80.3%-99.3%) (Figure 3B). The findings suggest that some of the anti-Spike IgG antibodies detected by the ELISA may lack neutralizing activity and therefore were not detected by SARS-CoV-2 bNAb assay[18]. Overall, these results demonstrate the reliability of the SARS-CoV-2 bNAb assay as an *in vitro* platform for detecting serum NAbs.

Identification of broadly neutralizing monoclonal Abs against SARS-CoV-2 variants

To demonstrate the application of SARS-CoV-2 bNAb assay in identifying monoclonal NAbs for potential treatment purposes, we tested six anti-Spike antibodies that are available in the laboratory[19] (Figure 4A). The results revealed that three antibodies (#26, #20, #21) have neutralizing activity. Antibodies #20 and #21 inhibited ACE2 binding to D614G, Alpha, Beta, Kappa and Delta variants, but were not effective in inhibiting the ACE2 binding to the Omicron BA.1 variant. Antibody #26 exhibited the ability to inhibit Spike-ACE2 interactions for D614G, Alpha, Beta, Kappa,Delta and Omicron BA.1 variants.

Subsequently, the half-maximal inhibitory concentration (IC50) values were calculated and represented in a heatmap (Figure 4B). The results showed that antibody #26 possessed broad neutralizing activity to all tested SARS-CoV-2 variants (Kappa, D614G, Alpha, Delta, Beta, Omicron BA.1). The IC50 to D614G (0.47 µg/mL) was confirmed with ELISA (0.35 µg/mL) and pseudovirus neutralizing assay (0.21 µg/mL) in our previous work[19]. While the IC50 of antibody #26 to the Omicron variant was ten-fold lower than non-Omicron variants. These findings underscore the ability of our assay to rapidly screen for monoclonal NAbs with potential therapeutic applications.

Evaluation of serum NAbs in individuals receiving the third dose vaccination

We tested the serum NAbs from 56 individuals who received two doses of the inactivated vaccine (Sinovac-CoronaVac) and boosted with a third dose with either an inactivated vaccine or recombinant subunit vaccine (ZF2001) (Table 1)[20]. The inhibition rate (%) was calculated by deducting the background noise using 147 serum samples collected prior to the COVID-19 pandemic[21]. The results showed that the third dose vaccination elicited a strong protective immune response against the non-Omicron variants with the highest inhibition rate (%) of D614G, followed by Gamma, Alpha, Delta, and Kappa variants. Unfortunately, the inhibition rate (%) was much lower in Omicron BA.2 (0.44×), BA.1 (0.43×), BA.3 (0.41×), BA.5 (0.35×), and BA.4 (0.33×) variants, indicating the resistance of these variants to the Sinovac-CoronaVac vaccine and the ZF2001 vaccine (Figure 5A).

Furthermore, we compared the inhibition (%) of serum NAbs in individuals who received either a third dose of inactivated vaccine or recombinant vaccine; no significant difference was observed (Figure 5B). These findings highlight the immunological resistance of different SARS-CoV-2 variants to the Sinovac-CoronaVac and ZF2001 vaccines, and suggest the need for developing a new vaccine that provides broad protection against SARS-CoV-2 variants.

Discussion

In this work, we developed a high-throughput SARS-CoV-2 bNAb assay to detect a wide range of NAbs to non-Omicron and Omicron variants. Compared to the assay using Luminex technology[7, 8], our SARS-CoV-2 bNAb assay is 35-fold more sensitive, 2.5-fold less costly, and can be accessible to any laboratory that has a standard flow cytometer with the 532 nm and 635 nm lasers. Moreover, the simultaneous detection of NAbs to multiple SARS-CoV-2 variants can be achieved within a single experiment, and the assay can be periodically updated to include new variants. The reliability of NAb detection using our SARS-CoV-2 bNAb assay is demonstrated through comparisons with ELISA-based IgG serology and the cPass sVNT assay (Figure 3).

Using this platform, we constructed a comprehensive landscape of Spike trimer and ACE2 interactions for eleven SARS-CoV-2 VOCs (Figure 2). The results provide evidence that Omicron BA.1 showed the strongest binding affinity to the ACE2 receptor [22, 23]. Notably, the transmission rate of SARS-CoV-2 and its variants is dependent on numerous factors, including immune resistance, toxicity, etc[24].

Furthermore, our investigation of serum NAbs in vaccinated individuals showed that the third dose of the inactivated vaccine or recombinant RBD vaccine resulted in a strong inhibition of Spike-ACE2 interactions to the non-Omicron VOCs (D614G, Alpha, Beta, Gamma,

Kappa). However, the protection was significantly decreased for Omicron VOCs (BA.2, BA.1, BA.3, BA.5, BA.4) (Figure 5). These results demonstrate the significance of our proteomics platform in evaluating the broad protective activity of COVID-19 vaccines, which can guide the development of COVID-19 vaccines.

It is important to acknowledge some limitations of our study. First, the *in vitro* detection of NAbs may not represent viral neutralization *in vivo*, although previously reported evidence has shown a good correlation between NAbs detected *in vitro* and *vivo*[5-8]. Second, the relationship between the inhibition levels obtained with the SARS-CoV-2 bNAb assay and the SARS-CoV-2 remains unclear. Third, the number of clinical samples employed in this study was limited, and the assay should be executed in a larger cohort to determine the NAb levels induced by different vaccines and infection with SARS-CoV-2 variants.

Conclusion

We have successfully developed and validated a high-throughput proteomics platform, enabling the comprehensive evaluation of NAbs against a wide range of SARS-CoV-2 VOCs. This platform offers an efficient, sensitive, and cost-effective approach for detecting broad NAbs within the population, providing an opportunity to guide the

design and evaluation of vaccines with enhanced protective efficacy against evolving SARS-CoV-2 strains. Overall, our work contributes to the ongoing efforts in combating the COVID-19 pandemic and advancing our understanding of immune responses to SARS-CoV-2.

References

1. The, L., The COVID-19 pandemic in 2023: far from over. *Lancet* **2023,** *401* (10371), 79.
2. Khoury, D. S.; Docken, S. S.; Subbarao, K.; Kent, S. J.; Davenport, M. P.; Cromer, D., Predicting the efficacy of variant-modified COVID-19 vaccine boosters. *Nat Med* **2023,** *29* (3), 574-578.
3. Ma, Y.; Deng, J.; Liu, Q.; Du, M.; Liu, M.; Liu, J., Long-Term Consequences of Asymptomatic SARS-CoV-2 Infection: A Systematic Review and Meta-Analysis. *Int J Environ Res Public Health* **2023,** *20* (2).
4. Thaweethai, T.; Jolley, S. E.; Karlson, E. W.; Levitan, E. B.; Levy, B.; McComsey, G. A.; McCorkell, L.; Nadkarni, G. N.; Parthasarathy, S.; Singh, U.; Walker, T. A.; Selvaggi, C. A.; Shinnick, D. J.; Schulte, C. C. M.; Atchley-Challenner, R.; Alba, G. A.; Alicic, R.; Altman, N.; Anglin, K.; Argueta, U.; Ashktorab, H.; Baslet, G.; Bassett, I. V.; Bateman, L.; Bedi, B.; Bhattacharyya, S.; Bind, M. A.; Blomkalns, A. L.; Bonilla, H.; Bush, P. A.; Castro, M.; Chan, J.; Charney, A. W.; Chen, P.; Chibnik, L. B.; Chu, H. Y.; Clifton, R. G.; Costantine, M. M.; Cribbs, S. K.; Davila Nieves, S. I.; Deeks, S. G.; Duven, A.; Emery, I. F.; Erdmann, N.; Erlandson, K. M.; Ernst, K. C.; Farah-Abraham, R.; Farner, C. E.; Feuerriegel, E. M.; Fleurimont, J.; Fonseca, V.; Franko, N.; Gainer, V.; Gander, J. C.; Gardner, E. M.; Geng, L. N.; Gibson, K. S.; Go, M.; Goldman, J. D.; Grebe, H.; Greenway, F. L.; Habli, M.; Hafner, J.; Han, J. E.; Hanson, K. A.; Heath, J.; Hernandez, C.; Hess, R.; Hodder, S. L.; Hoffman, M. K.; Hoover, S. E.; Huang, B.; Hughes, B. L.; Jagannathan, P.; John, J.; Jordan, M. R.; Katz, S. D.; Kaufman, E. S.; Kelly, J. D.; Kelly, S. W.; Kemp, M. M.; Kirwan, J. P.; Klein, J. D.; Knox, K. S.; Krishnan, J. A.; Kumar, A.; Laiyemo, A. O.; Lambert, A. A.; Lanca, M.; Lee-Iannotti, J. K.; Logarbo, B. P.; Longo, M. T.; Luciano, C. A.; Lutrick, K.; Maley, J. H.; Marathe, J. G.; Marconi, V.; Marshall, G. D.; Martin, C. F.; Matusov, Y.; Mehari, A.; Mendez-Figueroa, H.; Mermelstein, R.; Metz, T. D.; Morse, R.; Mosier, J.; Mouchati, C.; Mullington, J.; Murphy, S. N.; Neuman, R. B.; Nikolich, J. Z.; Ofotokun, I.; Ojemakinde, E.; Palatnik, A.; Palomares, K.; Parimon, T.; Parry, S.; Patterson, J. E.; Patterson, T. F.; Patzer, R. E.; Peluso, M. J.; Pemu, P.; Pettker, C. M.; Plunkett, B. A.; Pogreba-Brown, K.; Poppas, A.; Quigley, J. G.; Reddy, U.; Reece, R.; Reeder, H.; Reeves, W. B.; Reiman, E. M.; Rischard, F.; Rosand, J.; Rouse, D. J.; Ruff, A.; Saade, G.; Sandoval, G. J.; Schlater, S. M.; Shepherd, F.; Sherif, Z. A.; Simhan, H.; Singer, N. G.; Skupski, D. W.; Sowles, A.; Sparks, J. A.; Sukhera, F. I.; Taylor, B. S.; Teunis, L.;

345 Thomas, R. J.; Thorp, J. M.; Thuluvath, P.; Ticotsky, A.; Tita, A. T.; Tuttle, K. R.;
346 Urdaneta, A. E.; Valdivieso, D.; VanWagoner, T. M.; Vasey, A.; Verduzco-Gutierrez, M.;
347 Wallace, Z. S.; Ward, H. D.; Warren, D. E.; Weiner, S. J.; Welch, S.; Whiteheart, S. W.;
348 Wiley, Z.; Wisnivesky, J. P.; Yee, L. M.; Zisis, S.; Horwitz, L. I.; Foulkes, A. S.;
349 Consortium, R., Development of a Definition of Postacute Sequelae of SARS-CoV-2 Infection.
350 *JAMA* **2023**.
351 5. Nie, J.; Li, Q.; Wu, J.; Zhao, C.; Hao, H.; Liu, H.; Zhang, L.; Nie, L.; Qin, H.;
352 Wang, M.; Lu, Q.; Li, X.; Sun, Q.; Liu, J.; Fan, C.; Huang, W.; Xu, M.; Wang, Y.,
353 Quantification of SARS-CoV-2 neutralizing antibody by a pseudotyped virus-based assay. *Nat*
354 *Protoc* **2020,** *15* (11), 3699-3715.
355 6. Tan, C. W.; Chia, W. N.; Qin, X.; Liu, P.; Chen, M. I.; Tiu, C.; Hu, Z.; Chen, V.
356 C.; Young, B. E.; Sia, W. R.; Tan, Y. J.; Foo, R.; Yi, Y.; Lye, D. C.; Anderson, D. E.;
357 Wang, L. F., A SARS-CoV-2 surrogate virus neutralization test based on antibody-mediated
358 blockage of ACE2-spike protein-protein interaction. *Nat Biotechnol* **2020,** *38* (9), 1073-1078.
359 7. Fenwick, C.; Turelli, P.; Pellaton, C.; Farina, A.; Campos, J.; Raclot, C.; Pojer, F.;
360 Cagno, V.; Nussle, S. G.; D'Acremont, V.; Fehr, J.; Puhan, M.; Pantaleo, G.; Trono, D.,
361 A high-throughput cell- and virus-free assay shows reduced neutralization of SARS-CoV-2
362 variants by COVID-19 convalescent plasma. *Sci Transl Med* **2021,** *13* (605).
363 8. Lynch, K. L.; Zhou, S.; Kaul, R.; Walker, R.; Wu, A. H., Evaluation of Neutralizing
364 Antibodies against SARS-CoV-2 Variants after Infection and Vaccination Using a Multiplexed
365 Surrogate Virus Neutralization Test. *Clin Chem* **2022,** *68* (5), 702-712.
366 9. Perkmann, T.; Mucher, P.; Osze, D.; Muller, A.; Perkmann-Nagele, N.; Koller, T.;
367 Radakovics, A.; Flieder, I.; Repl, M.; Marculescu, R.; Wolzt, M.; Wagner, O. F.;
368 Binder, C. J.; Haslacher, H., Comparison of five Anti-SARS-CoV-2 antibody assays across three
369 doses of BNT162b2 reveals insufficient standardization of SARS-CoV-2 serology. *J Clin Virol*
370 **2023,** *158*, 105345.
371 10. Bal, A.; Pozzetto, B.; Trabaud, M. A.; Escuret, V.; Rabilloud, M.;
372 Langlois-Jacques, C.; Paul, A.; Guibert, N.; D'Aubarede-Frieh, C.;
373 Massardier-Pilonchery, A.; Fabien, N.; Goncalves, D.; Boibieux, A.; Morfin-Sherpa, F.;
374 Pitiot, V.; Gueyffier, F.; Lina, B.; Fassier, J. B.; Trouillet-Assant, S.; Group, C. S. S.,
375 Evaluation of High-Throughput SARS-CoV-2 Serological Assays in a Longitudinal Cohort of
376 Patients with Mild COVID-19: Clinical Sensitivity, Specificity, and Association with Virus
377 Neutralization Test. *Clin Chem* **2021,** *67* (5), 742-752.
378 11. Grant, R.; Sacks, J.; Abraham, P.; Chunsuttiwat, S.; Cohen, C.; Figueroa, J., When
379 to update COVID-19 vaccine composition. *Nature Medicine* **2023,** (29), 776–780.
380 12. Chao, Z.; Han, Y.; Jiao, Z.; You, Z.; Zhao, J., Prism Design for Spectral Flow
381 Cytometry. *Micromachines (Basel)* **2023,** *14* (2).
382 13. Yu, X.; Hartmann, M.; Wang, Q.; Poetz, O.; Schneiderhan-Marra, N.; Stoll, D.;
383 Kazmaier, C.; Joos, T. O., microFBI: a microfluidic bead-based immunoassay for multiplexed
384 detection of proteins from a microL sample volume. *PLoS One* **2010,** *5* (10).
385 14. Wang, Q.; Guo, Y.; Iketani, S.; Nair, M. S.; Li, Z.; Mohri, H.; Wang, M.; Yu, J.;
386 Bowen, A. D.; Chang, J. Y.; Shah, J. G.; Nguyen, N.; Chen, Z.; Meyers, K.; Yin, M. T.;
387 Sobieszczyk, M. E.; Sheng, Z.; Huang, Y.; Liu, L.; Ho, D. D., Antibody evasion by
388 SARS-CoV-2 Omicron subvariants BA.2.12.1, BA.4 and BA.5. *Nature* **2022,** *608* (7923),

389 603-608.
390 15. Mahalingam, G.; Arjunan, P.; Periyasami, Y.; Dhyani, A. K.; Devaraju, N.;
391 Rajendiran, V.; Christopher, A. C.; Kt, R. D.; Dhanasingh, I.; Thangavel, S.;
392 Murugesan, M.; Moorthy, M.; Srivastava, A.; Marepally, S., Correlating the differences in
393 the receptor binding domain of SARS-CoV-2 spike variants on their interactions with human
394 ACE2 receptor. *Sci Rep* **2023,** *13* (1), 8743.
395 16. Zhan, H.; Gao, H.; Liu, Y.; Zhang, X.; Li, H.; Li, X.; Wang, L.; Li, C.; Li, B.;
396 Wang, Y.; Dai, E.; Li, Y., Booster shot of inactivated SARS-CoV-2 vaccine induces potent
397 immune responses in people living with HIV. *J Med Virol* **2023,** *95* (1), e28428.
398 17. Marien, J.; Michiels, J.; Heyndrickx, L.; Nkuba-Ndaye, A.; Ceulemans, A.;
399 Bartholomeeusen, K.; Madinga, J.; Mbala-Kingebeni, P.; Vanlerberghe, V.;
400 Ahuka-Mundeke, S.; Wang, L. F.; Arien, K. K., Evaluation of a surrogate virus neutralization
401 test for high-throughput serosurveillance of SARS-CoV-2. *J Virol Methods* **2021,** *297*, 114228.
402 18. Chen, Y.; Zhao, X.; Zhou, H.; Zhu, H.; Jiang, S.; Wang, P., Broadly neutralizing
403 antibodies to SARS-CoV-2 and other human coronaviruses. *Nat Rev Immunol* **2023,** *23* (3),
404 189-199.
405 19. Liang, T.; Cheng, M.; Teng, F.; Wang, H.; Deng, Y.; Zhang, J.; Qin, C.; Guo, S.;
406 Zhao, H.; Yu, X., Proteome-wide epitope mapping identifies a resource of antibodies for
407 SARS-CoV-2 detection and neutralization. *Signal Transduct Target Ther* **2021,** *6* (1), 166.
408 20. Zhao, X.; Zhang, R.; Qiao, S.; Wang, X.; Zhang, W.; Ruan, W.; Dai, L.; Han, P.;
409 Gao, G. F., Omicron SARS-CoV-2 Neutralization from Inactivated and ZF2001 Vaccines. *N Engl*
410 *J Med* **2022,** *387* (3), 277-280.
411 21. Zhang, J.; Teng, F.; Zhang, X.; Wang, H.; Liang, T.; Guo, S.; Yu, X.,
412 Down-regulation of SARS-CoV-2 neutralizing antibodies in vaccinated smokers. *MedComm*
413 *(2020)* **2022,** *3* (3), e166.
414 22. Yin, W.; Xu, Y.; Xu, P.; Cao, X.; Wu, C.; Gu, C.; He, X.; Wang, X.; Huang, S.;
415 Yuan, Q.; Wu, K.; Hu, W.; Huang, Z.; Liu, J.; Wang, Z.; Jia, F.; Xia, K.; Liu, P.;
416 Wang, X.; Song, B.; Zheng, J.; Jiang, H.; Cheng, X.; Jiang, Y.; Deng, S. J.; Xu, H. E.,
417 Structures of the Omicron spike trimer with ACE2 and an anti-Omicron antibody. *Science*
418 **2022,** *375* (6584), 1048-1053.
419 23. Ma, W.; Fu, H.; Jian, F.; Cao, Y.; Li, M., Immune evasion and ACE2 binding affinity
420 contribute to SARS-CoV-2 evolution. *Nat Ecol Evol* **2023**.
421 24. Markov, P. V.; Katzourakis, A.; Stilianakis, N. I., Antigenic evolution will lead to new
422 SARS-CoV-2 variants with unpredictable severity. *Nat Rev Microbiol* **2022,** *20* (5), 251-252.
423 25. Zhang, X.; Zheng, M.; Wang, H.; Zhou, H.; Liang, T.; Zhang, J.; Ren, J.; Peng,
424 H.; Li, S.; Bian, H.; Wei, C.; Yin, S.; He, C.; Han, Y.; Li, M.; Hou, X.; Zhang, J.;
425 Xie, L.; Lv, J.; Kan, B.; Wang, Y.; Yu, X., Inhibitor screening using microarray identifies
426 the high capacity of neutralizing antibodies to Spike variants in SARS-CoV-2 infection and
427 vaccination. *Theranostics* **2022,** *12* (6), 2519-2534.
428 26. Yang, L.; Yu, Y.; Ma, C.; Wang, H.; Dai, J.; Duan, H.; Fu, Z.; Wu, P.; Wang,
429 D.; Yu, X., Development of RBC Membrane Antigen Arrays for Validating Blood Grouping
430 Reagents. *J Proteome Res* **2018,** *17* (9), 3237-3245.
431 27. Robin, X.; Turck, N.; Hainard, A.; Tiberti, N.; Lisacek, F.; Sanchez, J. C.; Muller,
432 M., pROC: an open-source package for R and S+ to analyze and compare ROC curves. *BMC*

Bioinformatics **2011**, *12*, 77.

Contributions

X.Z. and D.H. executed the experiments; M.L., X. Z., X.Z., X.X., T. L., and Y. Z. performed the data analysis; H.L. and Y.W. provided the clinical samples. X.Y., Y. L., and B.W. wrote the manuscript.

Acknowledgment

This work was supported by the Beijing Municipal Natural Science Foundation (M21003 and M23010), National Key R&D Program of China(2022YFE0210400, 2021YFA1301604, 2020YFE0202200), State Key Laboratory of Proteomics (SKLP-O202007), Academic leader of high-level public health technical personnel construction project of Beijing Municipal Health Commission (2022-2-014), Guangdong Province Science and Technology Planning Project (2020B1111100006), Innovation Team and Talents Cultivation Program of National Administration of Traditional Chinese Medicine. (No: ZYYCXTD-C-202204). We also thank Dr. Brianne Petritis for her critical review and editing of this manuscript.

Declaration of Interest Statement

The authors have declared no conflict of interest.

Supplementary materials

Supplementary Figure 1

Tables

Table 1. Clinical serum samples employed in this study

		3rd dose vaccination cohort (n=56)
Gender		
	Male	16(28.6%)
	Female	40(71.4%)
Age (years)		
	Range	21-70
	≤50	50(89.3%)
	> 50	6(10.7%)
Vaccination type		
Recombinant RBD-subunit vaccine (ZF2001)		38(83.9%)
Inactivated vaccine (Sinovac-CoronaVac)		18(16.1%)
Days of serum collection after 3rd dose vaccination		28

Figure legends

Figure 1. Schematic illustration of the high throughput SARS-CoV-2 bNAb assay. (A) Workflow of the SARS-CoV-2 bNAb assay. The beads coupled with SARS-CoV-2 VOC Spike trimer proteins are incubated with NAbs. The NAbs with neutralizing activity will block the Spike interaction with biotinylated ACE2 and SA-PE. The signal intensities of the Spike trimer-ACE2 interaction are inversely proportional to the level of NAbs. (B) Dose relationship curve of Spike-ACE2 interactions using Wellgrow and Luminex platforms. MFI = mean fluorescence intensity. (C) A comparison of the sensitivity to

detect Spike-ACE2 interactions with the Wellgrow and Luminex platforms.

Figure 2. Spike trimer-ACE2 interactions across different SARS-CoV-2 VOCs and ACE2 concentrations. (A) Dose relationship curve of the interactions between ACE2 and six SARS-CoV-2 non-Omicron VOCs and five Omicron VOCs. The x-axis represents the concentrations of the host ACE2 receptor. The y-axis represents the median of fluorescent signal intensity (MFI) of the SARS-CoV-2 Spike trimer-ACE2 interaction. N = nucleocapsid protein, which was used as a negative control. (B) Distribution of the NAb resistance to SARS-CoV-2 VOCs. The x-axis represents the SARS-CoV VOCs. The y-axis represents the EC50 calculated from SARS-CoV-2 VOC Spike-ACE2 interactions.

Figure 3. Comparison of the SARS-CoV-2 bNAb assay results with results from ELISA-based IgG serology and sVNT assays. (A) Correlation analysis of serological IgG detection between the SARS-CoV-2 bNAb assay and an ELISA-based IgG serology. (B) Correlation analysis of NAb detection using the SARS-CoV-2 bNAb assay and the FDA-approved cPass sVNT test. Six anti-Spike antibodies to SARS-CoV-2 Spike variants were analyzed with all

assays. The inhibition rate (%) was calculated using the signal from Spike trimer-ACE2 binding with and without serum NAbs. The concordance of NAb detection using the ELISA and sVNT assays was calculated as the positive and negative percent agreement (PPA and NPA, respectively). The blue and red dots represent positive (neutralizing activity) and negative (non-neutralizing) cases as determined by the comparative analysis, respectively.

Figure 4. Identification of monoclonal Abs with broad neutralizing capability. (A) Dose relationship curve demonstrating the ability of the NAb to inhibit SARS-CoV-2 VOC Spike trimer-ACE2 interactions. The x-axis represents the concentrations of the NAb. The y-axis represents the inhibition rate (%) of the NAb. N = nucleocapsid protein, which was used as a negative control. (B) Heatmap showing the IC50 of NAbs against different SARS-CoV-2 variants.

Figure 5. Detection of serum NAbs in vaccinated individuals. (A, B) Boxplot showing the distribution of inhibition rate (%) of serum NAbs against SARS-CoV VOCs in 56 vaccinated individuals. (B) Comparison of NAbs produced between groups receiving the inactivated vaccine (Sinovac-CoronaVac) or recombinant subunit vaccine (ZF2001). The

significance was performed using the Student's *t*-test (p-value < 0.01). **, ***, and **** represent a p-value less than 0.01, 0.001, and 0.0001, respectively.

Materials and methods

Collection of clinical samples

Clinical serum samples were collected from Beijing Ditan Hospital 28 days after the third dose of the COVID-19 vaccine (Table 1). Whole blood was collected in a vacutainer tube, and the serum was obtained via centrifugation at 4,000 × g at room temperature for 10 minutes. The serum was then transferred to a clean tube and stored at -80 °C until use. This study was approved by the Ethics Committee of Beijing Ditan Hospital (No.2021-010-01), and an exemption of informed consent was obtained before sera collection[25].

Preparation of SARS-CoV-2 bNAb reagents

The SARS-CoV-2 bNAb assay was developed in ProteomicsEra Medical Co., Ltd (Beijing, China). Briefly, 3 μg Spike trimer proteins (Sino Biological. and ACROBiosystems; Beijing, China) were coupled to 10^6 beads (Shenzhen Wellgrow Technology Co., Ltd.; Beijing, China) as previously described [26]. First, the beads were activated with sulfo-N-hydroxysuccinimide (NHS) (Thermo Scientific, USA) (50

mg/mL) and 1-Ethyl-3-[3-dimethylaminopropyl]-carbodiimide hydrochloride (EDC) (Solarbio, Beijing, China) (50 mg/mL) by incubating at room temperature for 20 minutes.

After washing with 2-(N-morpholino) ethanesulfonic acid (MES) buffer (50 mM, pH 5.0), the beads were incubated with the purified Spike trimer proteins for 2.5 hours in MES buffer. After an additional wash, the beads were blocked with the blocking buffer (PBS pH 7.4，0.05% Tween-20, 1% BSA) and then the coated beads were stored at 2-8 °C with the storage buffer (PBS pH7.4，0.05% Tween-20, 0.1% BSA, 0.05% NaN_3).

Detection of Spike-ACE2 interactions using bead-based assays

The SARS-CoV VOC Spike trimer-coupled beads were incubated with the biotinylated ACE2 (Sino Biological) at 0, 0.014, 0.041, 0.123, 0.370, 1.111, 3.333, 10 μg/mL for 1 hour in a 96-well plate. After washing three times with PBST-B (PBS pH7.4，0.05% Tween-20, 0.1% BSA) , the Spike-ACE2 interaction was detected using 2 μg/mL SA-PE (Thermo Scientific, USA) for 30 minutes at room temperature, and the signal was read with the EasyCell flow cytometer (Shenzhen Wellgrow Technology Co., Ltd.) at 200 beads/region.

Detection of monoclonal NAbs using the SARS-CoV-2 bNAb assay

To detect monoclonal NAbs, the SARS-CoV-2 Spike trimer protein-coupled beads were incubated at different concentrations (0, 0.014, 0.041, 0.123, 0.370, 1.111, 3.333, 10 μg/mL) of anti-RBD antibodies (#26, #20, #21, #22, #23, #73) for 2 hours at room temperature. After washing the bead three times with PBST-B, the beads were incubated with the biotinylated ACE2 (0.5 μg/mL) for 1 hour at room temperature, and the binding of ACE2 to Spike trimer protein was detected using SA-PE (2 μg/mL) for 30 minutes at room temperature. Finally, the signal was read with the EasyCell flow cytometry (Wellgrow Technology Co., Ltd.) at 200 beads/region.

Detection of Serum NAbs using SARS-CoV-2 bNAb assay.

The serum samples were diluted to 1:20 with PBST-B and then incubated with the Spike trimer protein-coupled beads for 2 hours at room temperature. After washing twice with PBST-B, the beads were then incubated with the biotinylated ACE2 (0.5 μg/mL) and 2 μg/mL SA-PE for 1 hour at room temperature. The signal was read with the EasyCell flow cytometer (Wellgrow Technology Co., Ltd.) at 200 beads/region.

Data analysis

To compare the inhibition rate (%) of serum NAbs against the D614G variant and other SARS-CoV-2 variants, the raw inhibition rates of different variants were first normalized using minimum-maximum normalization. Statistical analyses were performed using Student's *t*-test, with a p-value $\leq$ 0.01 considered as statistically significant. Correlations between the SARS-CoV-2 bNAb, ELISA-based serology test, and the cPass sVNT test were determined using Pearson correlation coefficients. Positive and negative percent agreement (PPA, NPA) were performed using the positive and negative judgment results from ELISA-based IgG serology and cPass sVNT tests. Ideal cutoffs for the SARS-CoV-2 bNAb method that maximized PPA and NPA were calculated using the Youden Index, which was implemented in the R package pROC (v 1.18.2) [27]. All data analyses were carried out in R (v4.2.3) under the R studio (v 19.1.3) environment.

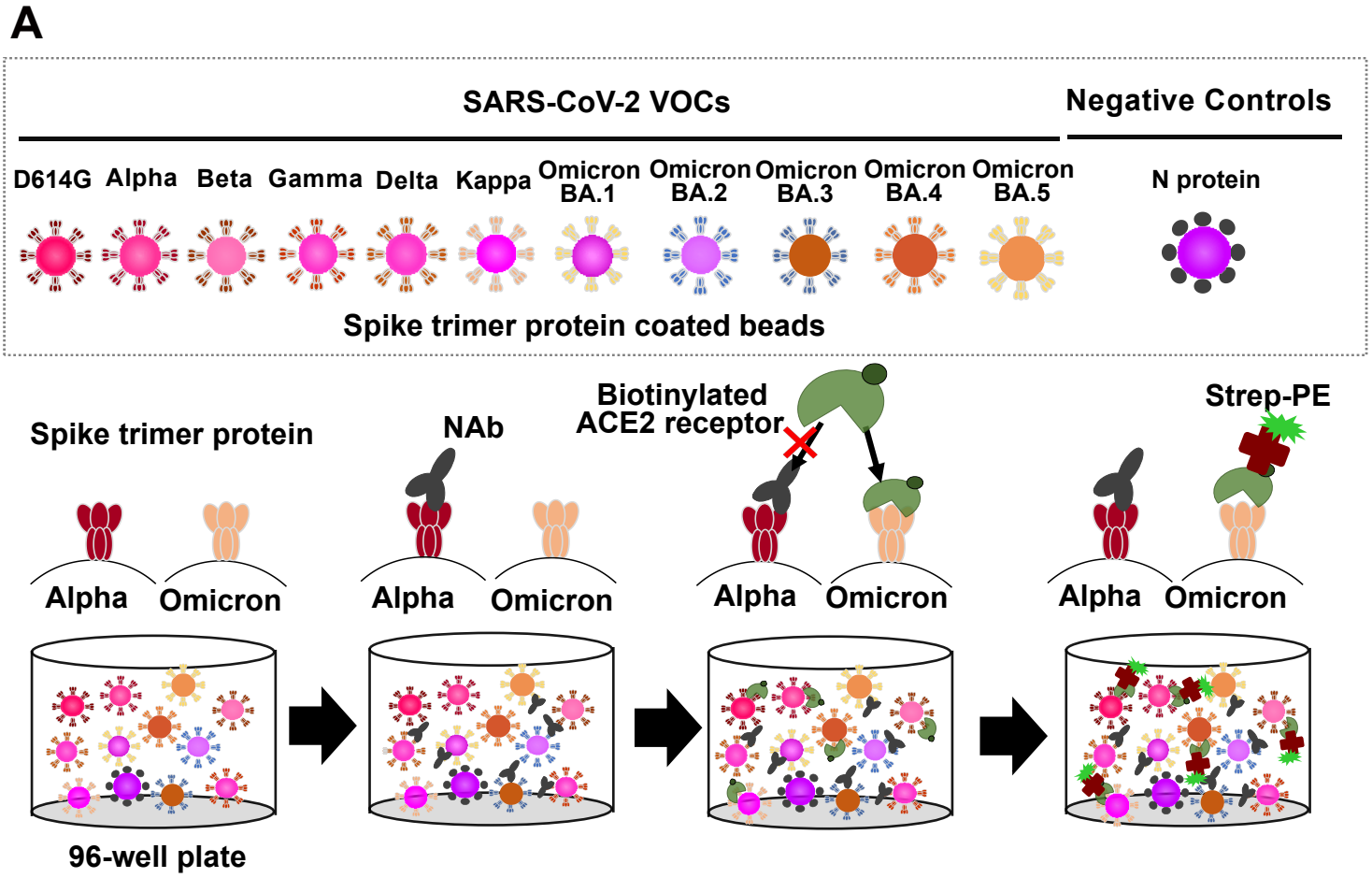

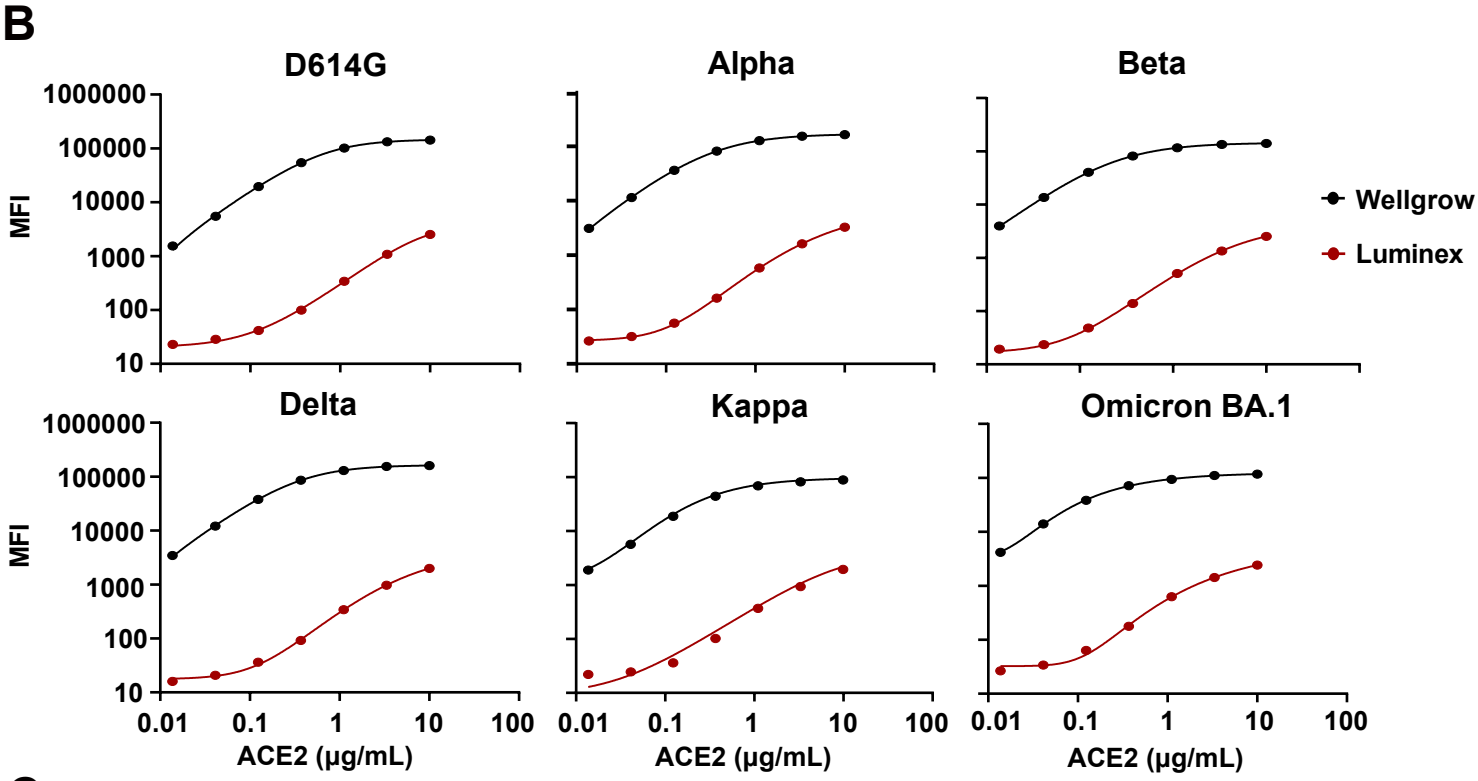

C

LOD [μg/mL]	D614G	Alpha	Beta	Delta	Kappa	Omicron BA.1	Average
Luminex	0.19	0.12	0.16	0.23	0.14	0.12	0.16
Wellgrow	0.006	0.003	0.005	0.003	0.007	0.008	0.005
Fold change [L/W] (×)	31.67	40	32	76.67	20	15	35.89±57.80 [-21.91～93.69]

A

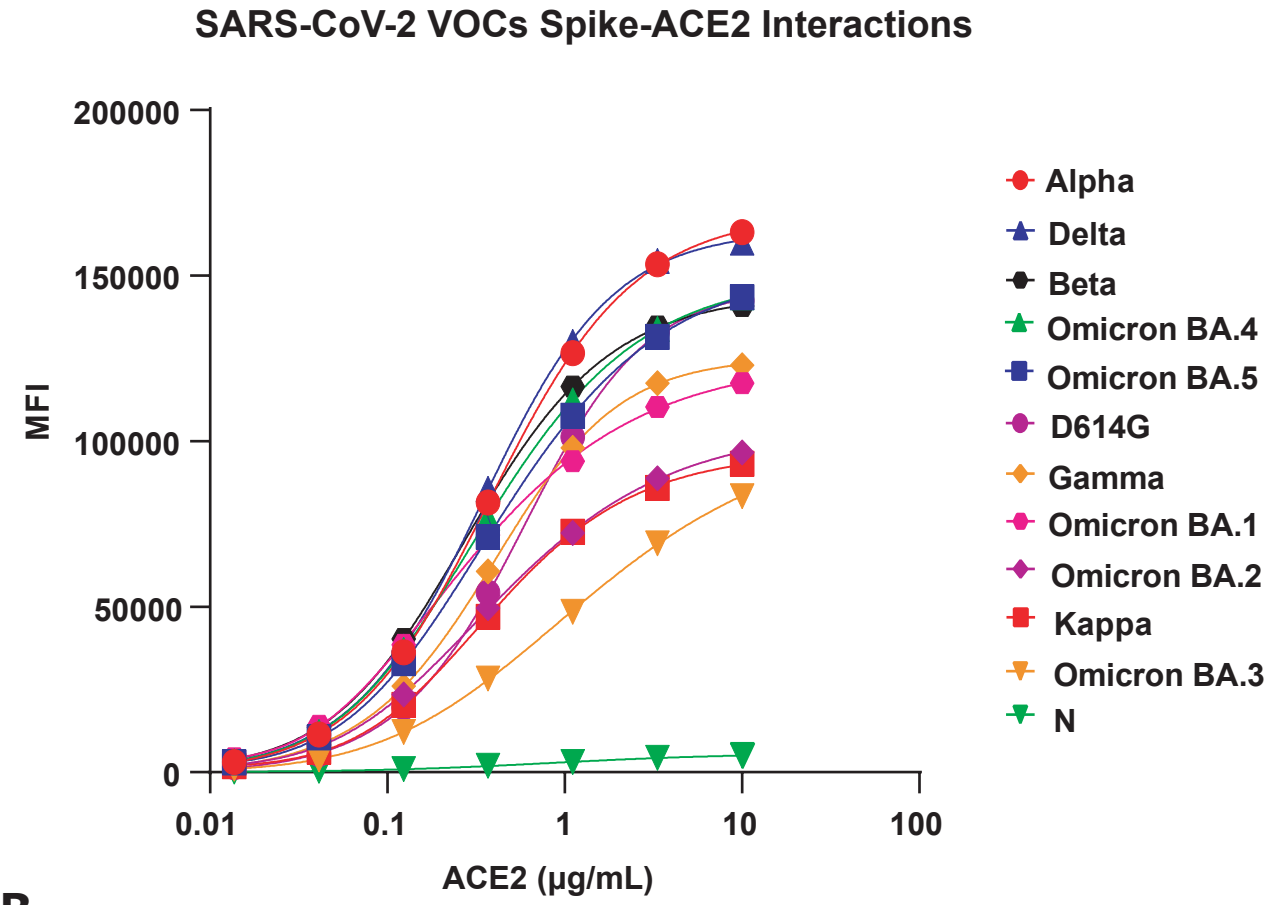
SARS-CoV-2 VOCs Spike-ACE2 Interactions
MFI
200000
150000
100000
50000
0
0.01
0.1
1
10
100
ACE2 (µg/mL)
Alpha
Delta
Beta
Omicron BA.4
Omicron BA.5
D614G
Gamma
Omicron BA.1
Omicron BA.2
Kappa
Omicron BA.3
N

B

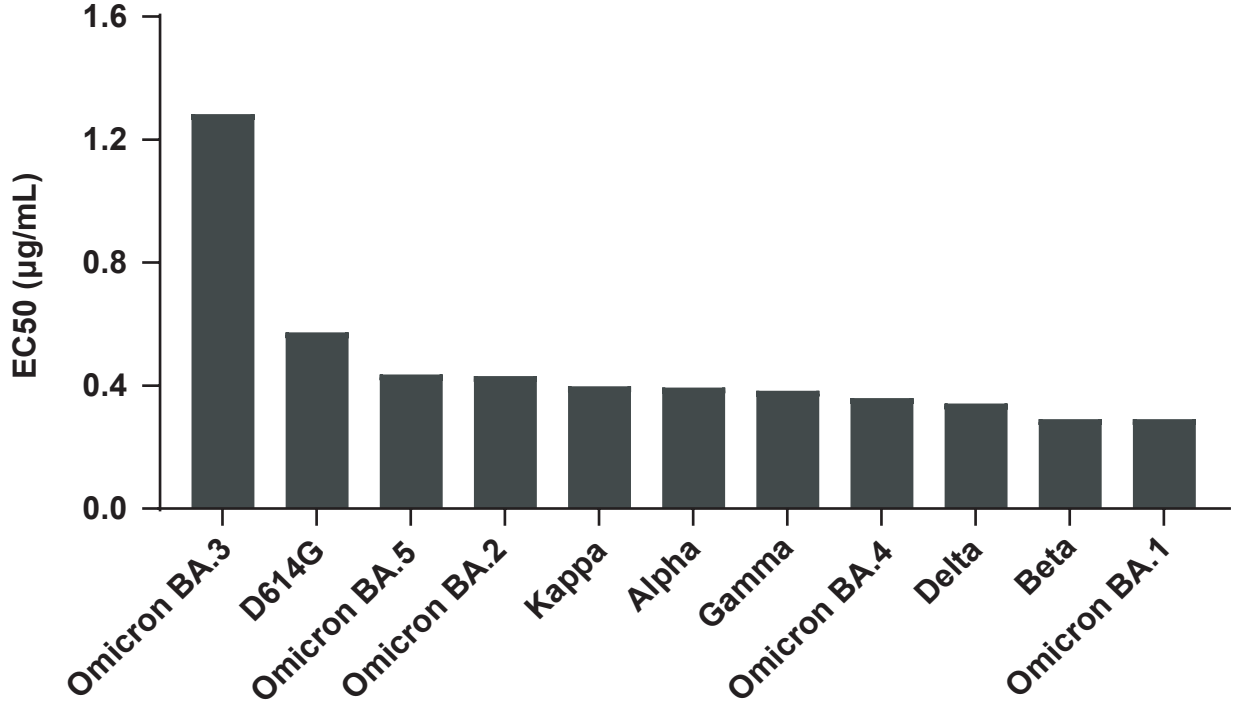
EC50 (µg/mL)
1.6
1.2
0.8
0.4
0.0
Omicron BA.3
D614G
Omicron BA.5
Omicron BA.2
Kappa
Alpha
Gamma
Omicron BA.4
Delta
Beta
Omicron BA.1

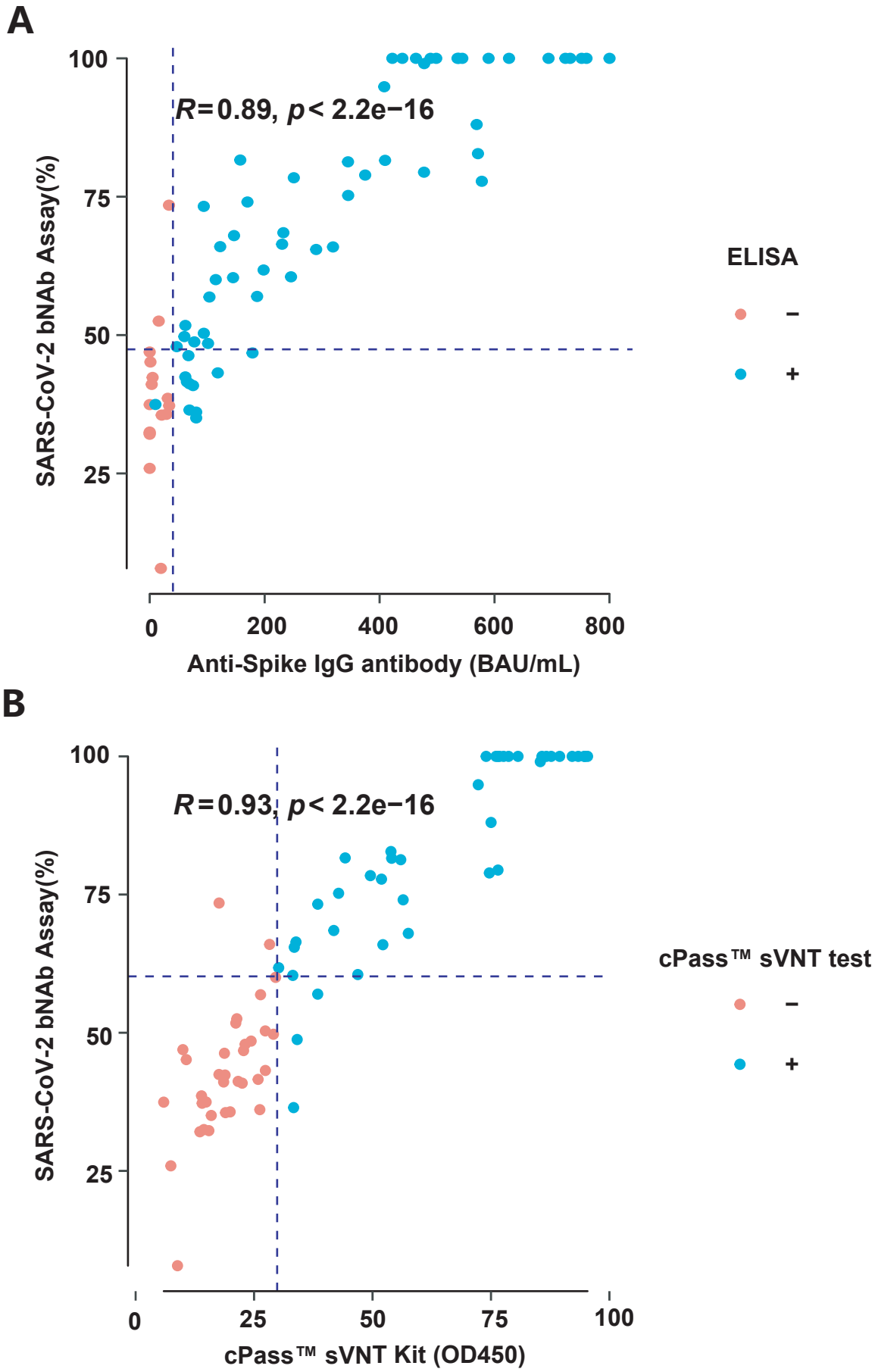

PPA (%) (95% CI)	NPA (%) (95% CI)
92.7 (80.1-98.5)	94.1 (80.3-99.3)

A

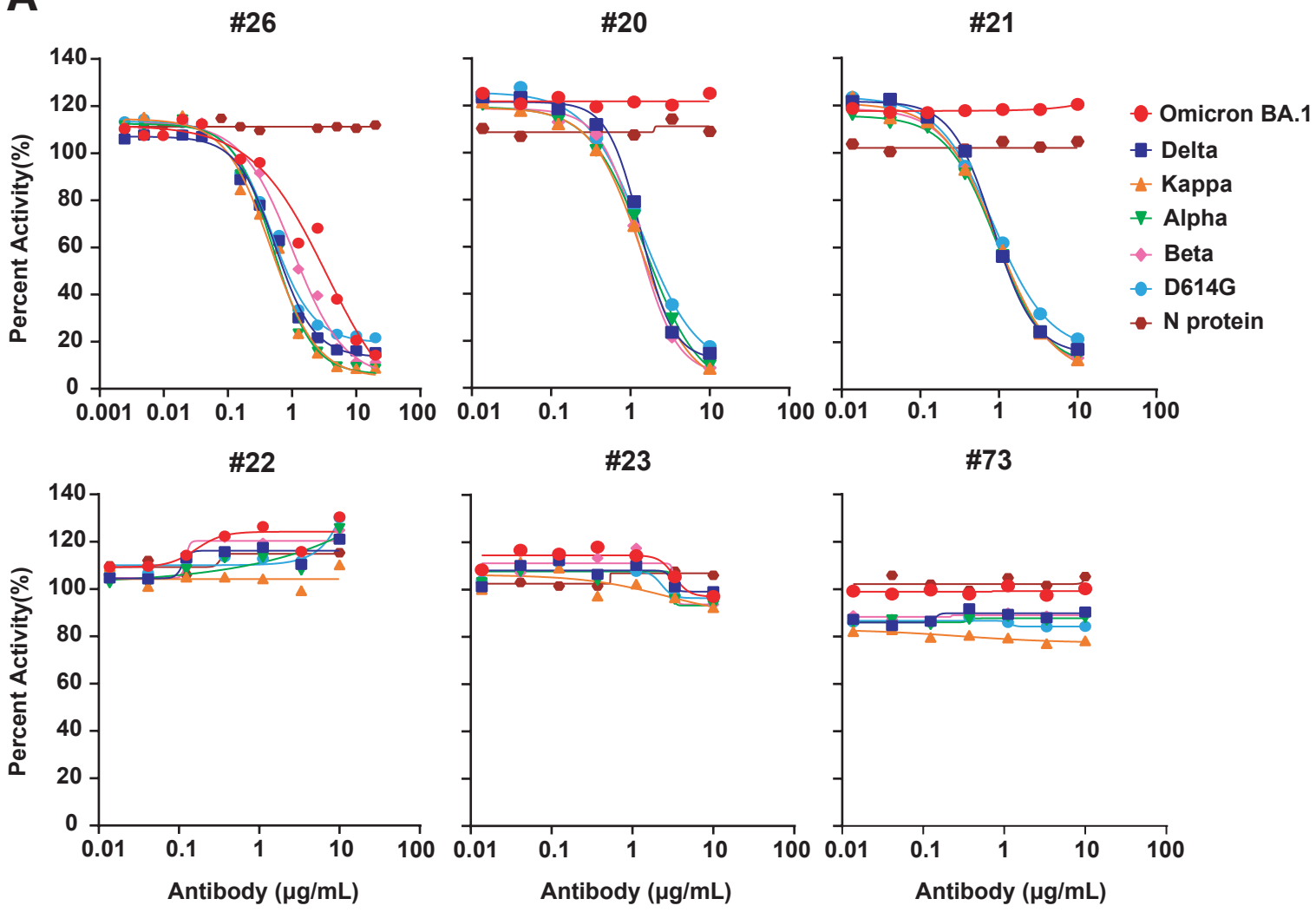

B

Antibody	D614G	Alpha	Beta	Delta	Kappa	Omicron BA.1
#26	0.4739	0.511	1.021	0.5504	0.468	3.429
#20	1.365	1.524	1.266	1.343	1.324	> 10
#21	0.8505	0.9199	0.8998	0.8429	0.9445	> 10
#22	> 10	> 10	> 10	> 10	> 10	> 10
#23	> 10	> 10	> 10	> 10	> 10	> 10
#73	> 10	> 10	> 10	> 10	> 10	> 10

IC50 (μg/mL)

0 5 10

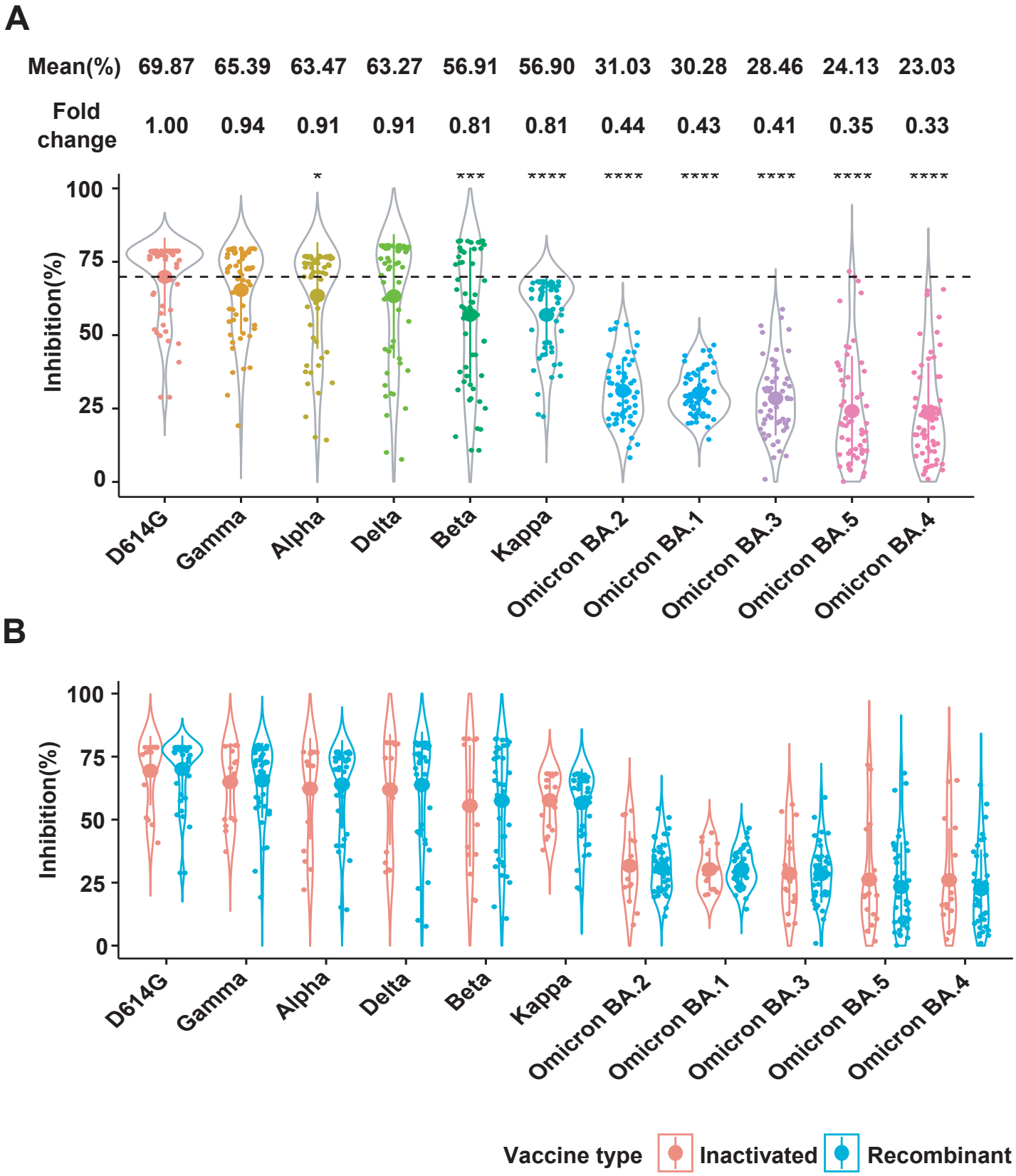
A
Mean(%) 69.87 65.39 63.47 63.27 56.91 56.90 31.03 30.28 28.46 24.13 23.03
Fold change 1.00 0.94 0.91 0.91 0.81 0.81 0.44 0.43 0.41 0.35 0.33
* *** **** **** **** **** **** ****
Inhibition(%)
100
75
50
25
0
D614G
Gamma
Alpha
Delta
Beta
Kappa
Omicron BA.2
Omicron BA.1
Omicron BA.3
Omicron BA.5
Omicron BA.4
B
Inhibition(%)
100
75
50
25
0
D614G
Gamma
Alpha
Delta
Beta
Kappa
Omicron BA.2
Omicron BA.1
Omicron BA.3
Omicron BA.5
Omicron BA.4
Vaccine type
Inactivated
Recombinant